


# Density control of GaN quantum dots on AlN single crystal

Cite as: Appl. Phys. Lett. **114**, 082101 (2019); <https://doi.org/10.1063/1.5083018>

Submitted: 27 November 2018 . Accepted: 16 January 2019 . Published Online: 25 February 2019

Sebastian Tamariz , Gordon Callsen , and Nicolas Grandjean 

## COLLECTIONS

 This paper was selected as Featured



View Online



Export Citation



CrossMark

## ARTICLES YOU MAY BE INTERESTED IN

[Non-uniform Mg distribution in GaN epilayers grown on mesa structures for applications in GaN power electronics](#)

Applied Physics Letters **114**, 082102 (2019); <https://doi.org/10.1063/1.5088168>

[Graphene-assisted quasi-van der Waals epitaxy of AlN film for ultraviolet light emitting diodes on nano-patterned sapphire substrate](#)

Applied Physics Letters **114**, 091107 (2019); <https://doi.org/10.1063/1.5081112>

[Highly radiative nature of ultra-thin c-plane Al-rich AlGaIn/AlN quantum wells for deep ultraviolet emitters](#)

Applied Physics Letters **114**, 102101 (2019); <https://doi.org/10.1063/1.5087543>

Applied Physics Reviews  
Now accepting original research

2017 Journal  
Impact Factor:  
**12.894**

# Density control of GaN quantum dots on AlN single crystal

Cite as: Appl. Phys. Lett. **114**, 082101 (2019); doi: [10.1063/1.5083018](https://doi.org/10.1063/1.5083018)

Submitted: 27 November 2018 · Accepted: 16 January 2019 ·

Published Online: 25 February 2019



View Online



Export Citation



CrossMark

Sebastian Tamariz,<sup>a)</sup>  Gordon Callsen,  and Nicolas Grandjean 

## AFFILIATIONS

Institute of Physics, Ecole Polytechnique Fédérale de Lausanne, EPFL, Station 3, CH-1015 Lausanne, Switzerland

<sup>a)</sup>[sebastian.tamariz@epfl.ch](mailto:sebastian.tamariz@epfl.ch)

## ABSTRACT

Full control over the density and emission properties of GaN quantum dots (QDs) should be feasible, provided that the growth proceeds in the Stranski-Krastanov (SK) growth mode. In this work, we derive the phase diagram for GaN QD formation on AlN by  $\text{NH}_3$ -molecular beam epitaxy and analyze the corresponding optical signature by micro-photoluminescence ( $\mu$ -PL). Interestingly, the growth window for SK-GaN QDs is very narrow due to the relatively small lattice mismatch of the GaN/AlN system (2.5%), constituting a fundamental challenge for QD growth control. By relying on bulk AlN single crystal substrates, we demonstrate QD density control over three orders of magnitude, from  $10^8$  to  $10^{11} \text{ cm}^{-2}$  by changing the growth rate. In contrast, the QD density is pinned to  $2 \times 10^{10} \text{ cm}^{-2}$  when growing on AlN/sapphire templates, which exhibit dislocation densities on the order of  $10^{10} \text{ cm}^{-2}$ . Thanks to QD densities as low as  $10^8 \text{ cm}^{-2}$  on bulk AlN, we can probe the emission of spatially isolated single GaN QDs by  $\mu$ -PL on unprocessed samples.

© 2019 Author(s). All article content, except where otherwise noted, is licensed under a Creative Commons Attribution (CC BY) license (<http://creativecommons.org/licenses/by/4.0/>). <https://doi.org/10.1063/1.5083018>

The progress in the field of integrated quantum optics has been fueled by potential applications in, e.g., quantum-computing and secure data transmission.<sup>1,2</sup> First, lab-on-a-chip experiments using the mature III-V quantum dot (QD) arsenide material system were realized to address, e.g., single photon emission characteristics,<sup>1</sup> two-photon interference,<sup>3</sup> and polarization entanglement.<sup>4</sup> Nowadays, all building blocks from the quantum light source, over waveguides<sup>5</sup> and beamsplitters,<sup>6,7</sup> to single photon detectors<sup>8</sup> are at hand. Epitaxial QDs have proven as promising quantum light emitters based on their scalability and integrability.<sup>2</sup> However, the operation of such sources is often limited to cryogenic temperatures.<sup>9</sup>

In contrast, future non-cryogenic on-chip quantum optics would need to build on nanostructures or suitable point-defects based on wide-bandgap materials such as SiC,<sup>10</sup> diamond,<sup>11</sup> II/III-oxides,<sup>12</sup> or III-nitrides. For instance, GaN QDs embedded in AlN can exhibit large exciton binding energies in excess of 150 meV, rendering them ideal candidates for single photon emission at room temperature and beyond.<sup>13</sup> Recently, coherent control of excitonic qubits,<sup>14</sup> two-photon emission at 50 K based on the biexciton cascade,<sup>15</sup> and room-temperature single photon emission<sup>16</sup> were reported for GaN QDs embedded in

Al(Ga)N. Single photon emission up to 350 K was reported by Holmes *et al.*<sup>17</sup> from a GaN QD embedded in a nano-pillar. Despite such recent achievements, future on-chip integration of three-dimensional (3D)-structures that boost the light out-coupling efficiency shall prove to be extremely challenging. The aforementioned complex arsenide structures are commonly based on planar, strain-induced Stranski-Krastanov (SK) QDs which can, e.g., straightforwardly be embedded into photonic crystals.<sup>2</sup> In the prototypical InAs/GaAs system, SK growth manifests itself by a spontaneous morphological transition from a smooth 2D surface to 3D islanding during growth after a certain thickness of InAs.<sup>18,19</sup> In this material system, the QD size and the density are tunable over a large range of values,<sup>20</sup> in part due to the large lattice mismatch of 7.2% between InAs and GaAs and the high surface kinetics, which favor islanding.

The lattice mismatch between GaN and AlN is only 2.5%, which may hinder the SK growth mode transition. Nonetheless, GaN/AlN QDs have been realized by using plasma assisted molecular beam epitaxy (PA-MBE),<sup>21-24</sup> ammonia molecular beam epitaxy ( $\text{NH}_3$ -MBE),<sup>25-29</sup> and metalorganic vapor phase epitaxy (MOVPE).<sup>30-32</sup> Based on these techniques, several growth methods for achieving QDs have been developed. For

instance, droplet epitaxy,<sup>33,34</sup> SK,<sup>22,24</sup> and modified-SK<sup>34,35</sup> growth were reported for PA-MBE. In the case of NH<sub>3</sub>-MBE, a transition from a 2D to a 3D growth mode was found for the growth of AlGaIn when finely tuning the growth conditions;<sup>36</sup> however, for the growth of GaN, most QD growths were achieved by a modified-SK method. A 2D-3D transition is achieved after a growth interruption and cutting off of the NH<sub>3</sub> flow.<sup>25-27,29,37</sup> Notice that all these different approaches share one common disadvantage: the QD density commonly appears to be pinned at about 10<sup>10</sup> cm<sup>-2</sup>, representing the lack of growth control necessary for further progress towards integrated quantum optic devices.

In the present work, we demonstrate GaN/AlN QD density control from 10<sup>8</sup> to 10<sup>11</sup> cm<sup>-2</sup> by using a SK growth mode on bulk AlN substrates. By comparing GaN QDs grown on bulk AlN and on AlN on sapphire templates, we demonstrate that the presence of threading dislocations fixes the minimum QD density which can be achieved on the latter. In contrast, growth on AlN single crystal substrates allows us to tune the QD density over three orders of magnitude, while keeping the same equivalent GaN coverage. Finally, we report the photoluminescence (PL) properties of low density QDs grown on the AlN single crystal substrate.

Growth was performed on AlN on *c*-plane sapphire with typical threading dislocation densities (TDDs) on the order of 10<sup>10</sup> cm<sup>-2</sup> and on a bulk AlN single crystal with TDD of 10<sup>3</sup> cm<sup>-2</sup> substrates in a Riber C-21 MBE. Prior to QD growth, 100 nm of AlN were grown at high temperatures (1050–1150 °C) under N-rich conditions (*V*/*III* ~ 200) to ensure a single monolayer (ML) height step flow morphology.<sup>38,39</sup> We define the following as the standard growth conditions for GaN QDs on AlN: a substrate temperature (*T*<sub>S</sub>) of 750 °C, a GaN growth rate (*V*<sub>GaN</sub>) of 0.025 ML/s, a GaN equivalent thickness (*h*) of 4 MLs, and an NH<sub>3</sub> beam equivalent pressure (BEP) of 3.3 × 10<sup>-7</sup> Torr (chamber pressure around 7 × 10<sup>-8</sup> Torr).

The film's free energy describing the formation of self-assembled 3D islands of GaN deposited on AlN can be expressed in terms of the energy of a pseudomorphic 2D surface and of the energy of coherently strained 3D islands. According to Mariette,<sup>40</sup> one obtains

$$E_{2D}(h) = M\epsilon_{\text{GaN}}^2 h + \gamma, \quad (1)$$

and

$$E_{3D}(h) = (1 - \alpha)M\epsilon_{\text{GaN}}^2 h + \gamma + \Delta\gamma, \quad (2)$$

where  $E_{2D}(h)$  is the energy of the pseudomorphic 2D surface,  $M$  is the film's biaxial modulus,  $\epsilon_{\text{GaN}}$  is the strain,  $M\epsilon_{\text{GaN}}^2 h$  is the elastic energy for a given GaN equivalent thickness ( $h$ ), and  $\gamma$  is the surface energy for the (0001) surface.  $E_{3D}(h)$  is the energy of the layer when a fraction  $\alpha$  of the surface is covered by 3D islands, and  $\Delta\gamma$  is the surface energy cost to form the 3D islands. For a given GaN thickness  $h$ , the layer will rearrange in 3D islands if  $E_{3D}(h) < E_{2D}(h)$  and the minimal thickness for which this inequality holds will be the critical thickness for the 2D-3D transition ( $h_{2D-3D}$ ). Furthermore, islanding supposes a sufficient diffusion length. The latter depends mainly on  $T_S$  and  $V_{\text{GaN}}$ . Hence, the formation of 3D islands is kinetically limited and higher  $T_S$  leads

to faster 3D islanding as shown by Damilano *et al.*<sup>26</sup> From this simplified model, it is already clear that  $\Delta\gamma$  plays a paramount role in determining whether the layer will undergo a 2D to 3D transition. For instance, using standard growth conditions in NH<sub>3</sub>-MBE, Damilano *et al.*<sup>25</sup> observed a 2D growth regime and plastic relaxation. This behavior occurs for a wide range of substrate temperatures and is independent of the initial density of dislocations.<sup>41</sup> A 2D-3D transition was only possible after a growth interruption without NH<sub>3</sub> flow—the basis for the modified SK-growth method. It was concluded that  $\Delta\gamma$  is reduced under vacuum; alternatively, this can be understood as  $\Delta\gamma$  being proportional to the NH<sub>3</sub> pressure. One could be tempted to increase  $T_S$  to provide the energy to promote island formation and overcome the barrier set by the surface energy. However, GaN decomposes under vacuum at a significant rate for temperatures above 750 °C, a process that can be prevented by supplying NH<sub>3</sub>.<sup>42</sup> In summary, we can establish the following guidelines for the spontaneous formation of self-assembled GaN 3D islands by a SK growth mode:

1.  $T_S$  should be increased to maximize the diffusion length but should be kept at reasonable values to prevent high evaporation rates ( $V_{\text{evaporation}}$ ).
2. The NH<sub>3</sub> flow should be minimized because  $\Delta\gamma$  depends strongly on the NH<sub>3</sub> pressure. Indeed, high NH<sub>3</sub> flows completely hinder the formation of 3D islands.<sup>25</sup>
3. The growth rate  $V_{\text{GaN}}$  should be low enough to allow the necessary formation time<sup>26</sup> for a given  $\Delta\gamma$  and  $T_S$ .  $V_{\text{GaN}}$  should also be lowered in order to remain under N-rich conditions, even when using low NH<sub>3</sub> flows.

With these considerations in mind, we selected a growth temperature of 750 °C and decreased both the growth rate (0.025 ML/s) and the NH<sub>3</sub>-BEP (3.3 × 10<sup>-7</sup> Torr), matching the standard growth conditions. The 2D-3D morphological transition was monitored by reflection high energy electron diffraction (RHEED). In Fig. 1(a), the typical RHEED intensity curves during the growth of GaN on AlN for growth conditions promoting 3D island formation are displayed. RHEED intensity oscillations, signature of a layer by layer growth mode, are observed for the specular beam for a thickness up to 3 MLs; afterwards, the oscillations stop and the intensity decreases. After the completion of 3 MLs, a drastic increase in intensity is observed at Bragg diffraction positions, indicating the formation of the 3D islands. The critical thickness for the morphological transition was further confirmed by atomic force microscopy (AFM). As shown in Figs. 1(b) and 1(c), a 2D-3D transition occurs at 3 MLs. Very small, low density (3 × 10<sup>9</sup> cm<sup>-2</sup>) QDs are obtained. The inset of Fig. 1(c) displays a height profile over an exemplary island.

Note that this transition occurs without growth and NH<sub>3</sub> interruption.<sup>25</sup> Thus, our results indicate that a conventional SK growth can be achieved by NH<sub>3</sub>-MBE. Hence, the versatile growth control found in arsenides<sup>20</sup> should become applicable for GaN/AlN QDs.

We report in Fig. 2 a phase diagram of the growth conditions that lead either to the spontaneous formation of 3D islands (red dots) or to a 2D surface (black crosses) on AlN/sapphire templates. Under high NH<sub>3</sub> BEP and low  $T_S$ , the RHEED shows

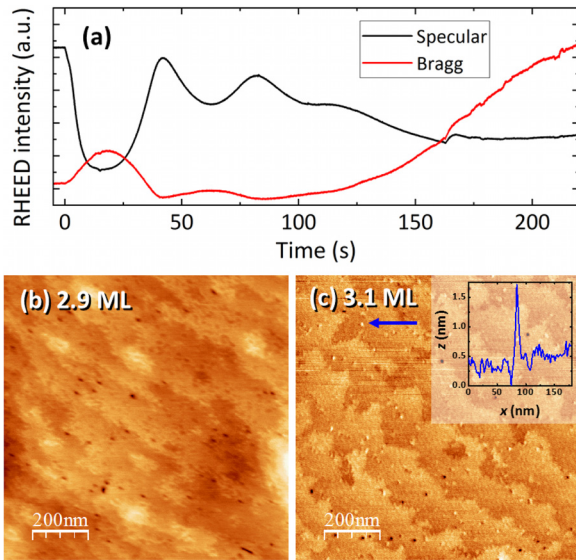


**FIG. 1.** (a) RHEED intensity at the specular and Bragg positions for standard growth conditions. (b) and (c)  $1 \times 1 \mu\text{m}^2$  AFM scans of GaN on AlN/sapphire templates, showcasing a value of 3 MLs for the critical thickness of the 2D-3D transition ( $h_{2D-3D}$ ). Inset: Height profile over a 3D island.

the common streaky pattern, which is typical for the 2D surface. The high  $\text{NH}_3$  pressure leads to high  $\Delta\gamma$  values that prevent islanding, and GaN relaxes plastically. In Fig. 2, this growth regime is indicated by blue color shading. At low  $\text{NH}_3$  BEP and high  $T_S$ ,  $V_{\text{evaporation}}$  is non-negligible and can compete with  $V_{\text{GaN}}$  (green shaded regime of Fig. 2). Thus, only a sharp growth window enables 3D islands. Further details are discussed in the [supplementary material](#).

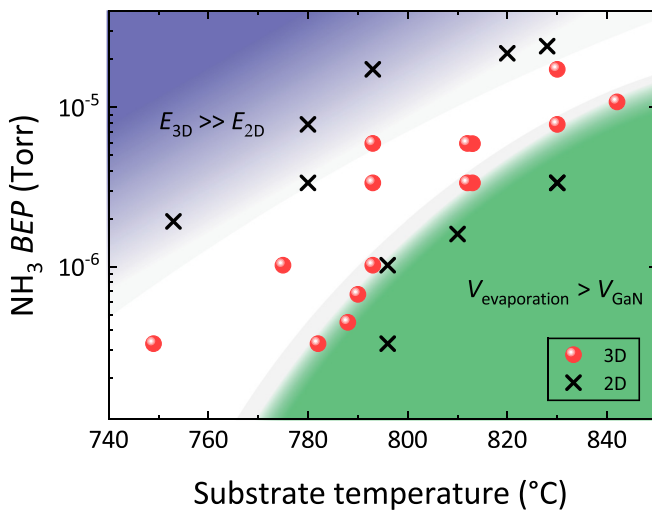


**FIG. 2.** Phase diagram of the surface morphology measured by RHEED in terms of  $\text{NH}_3$  beam equivalent pressure (BEP) and substrate temperature at a growth rate of 0.025 ML/s.

The equivalent GaN thickness  $h$  is the most prominent variable affecting the size and the density of the QDs. An increase in  $h$  simultaneously increases the QDs' density and height and thus decreases the emission energy.<sup>21,23,25,30</sup> While using standard growth conditions and  $h=4$  MLs, the AFM evidences well-defined QDs with a density of  $\sim 10^{10} \text{cm}^{-2}$  and typical heights and diameters of 2.5–3 nm and 20–35 nm, respectively. At 6 MLs, the surface is completely covered with QDs and the QD density reaches  $10^{11} \text{cm}^{-2}$  (see [supplementary material](#)).

An even more insightful observation regarding the evolution of the QD density on AlN/sapphire templates can be made by using our standard SK growth conditions at varying growth rates  $V_{\text{GaN}}$ . In general, longer diffusion lengths can be achieved by either increasing  $T_S$  or by decreasing  $V_{\text{GaN}}$ . A longer diffusion length should increase the probability for an ad-atom to attach at an existing QD site instead of nucleating a new island, thus reducing the density by increasing the QD size. However, in contrast to these expectations, AFM demonstrates that the QD density is hardly altered upon varying  $V_{\text{GaN}}$  (black squares in Fig. 3). The QD density appears as pinned to  $\approx 2 \times 10^{10} \text{cm}^{-2}$  when growing on AlN/sapphire templates in the investigated  $V_{\text{GaN}}$  interval (0.001–0.025 ML/s). Hence, even though the conventional SK growth mode is applied, QD density control is still not possible.

Interestingly, switching from AlN/sapphire templates to bulk AlN single crystal substrates provides further insight into the apparent growth limitations. In contrast to our previous observation, a strong dependence of the QD density on  $V_{\text{GaN}}$  is present when growing on AlN single crystal substrates (see Fig. 3—blue dots). AFM images 1–3 from Fig. 3 highlight the achieved QD growth control by varying  $V_{\text{GaN}}$ .

The dependence of the QD density on the substrate of choice can be understood by a detailed examination of AFM scan 4 from Fig. 4. Here, small dark spots can be observed next to most of the QDs. These pits are identified as edge dislocations. Such positioning of QDs next to edge dislocations was first

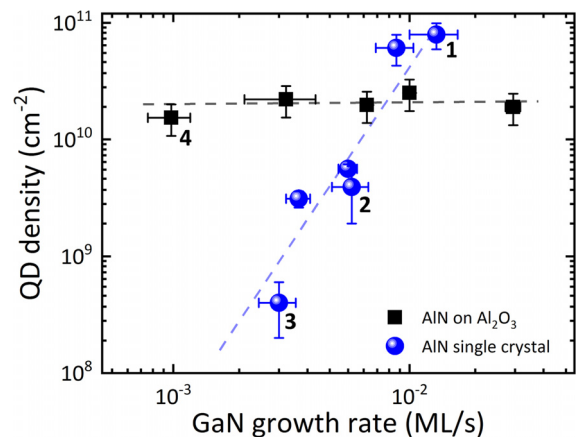


**FIG. 3.** QD density measured by AFM as a function of  $V_{\text{GaN}}$  on AlN/sapphire templates (black squares) and AlN single crystal substrates (blue dots). The dashed lines are guides to the eye. The numerical labels are related to the corresponding AFM images in Fig. 4.

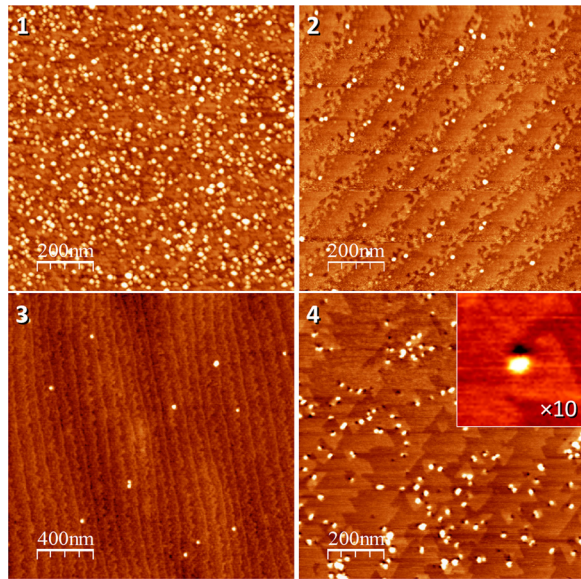


**FIG. 4.** AFM images of the labeled data points in Fig. 3. AFM images 1 to 3 originate from QD growth on AlN single crystal substrates, whereas image 4 originates from growth on an AlN/sapphire template. Inset: Magnification of a dot and a dislocation. Images 1, 2, and 4 show  $1 \times 1 \mu\text{m}^2$  areas, while AFM image 3 represents a  $2 \times 2 \mu\text{m}^2$  scan.

reported by Rouvière *et al.*<sup>43</sup> Edge dislocations create a strain dipole and thus provide a local minimum for strain release during the segregation of GaN.<sup>44,45</sup> Any structural defects will lead to a non-perfect strain field and thus to preferential nucleation sites for the QDs at the strain minima. In contrast, the close-to featureless surface of the AlN grown on the AlN single crystal substrates (except the atomic terraces) provides a very smooth, strain-induced potential landscape. Hence, the growth of low density QDs becomes feasible, provided a sufficient diffusion length, is applied.

In order to explore the optical properties of SK-GaN QDs grown on AlN single crystal substrates, we prepared a sample with parameters that lead to a very low QD density [ $h = 3.5$  ML and  $V_{\text{GaN}} = 0.0015 (\pm 0.0010)$  ML/s]. This sample was capped with a 50-nm thick AlN top barrier.

The sample was mapped using a 266 nm (4.66 eV) laser operating in continuous waves at a sample temperature of 5 K. A  $50 \times 50 \mu\text{m}^2$  map was obtained by moving the laser excitation spot using a step size of  $0.5 \mu\text{m}$  ( $\approx 0.5 \mu\text{m}$  laser excitation spot diameter). The polychromatic  $\mu$ -PL map scan is displayed in Fig. 5(a). The map is plotted such that it highlights deviations from the background luminescence within the 3.7 to 4.5 eV range. It becomes clear that only a low density of specific locations shows QD-like luminescence as demonstrated in Fig. 5(b). Here, a selection of typical QD spectra is shown, exhibiting distinct sharp emission lines. Given the low excitation power density applied for the map scan, it seems plausible as a first approximation that each emission line corresponds to a single QD.<sup>13,15</sup> Clearly, a pronounced contribution of multi-excitonic features is only expected for higher excitation densities. Based on this

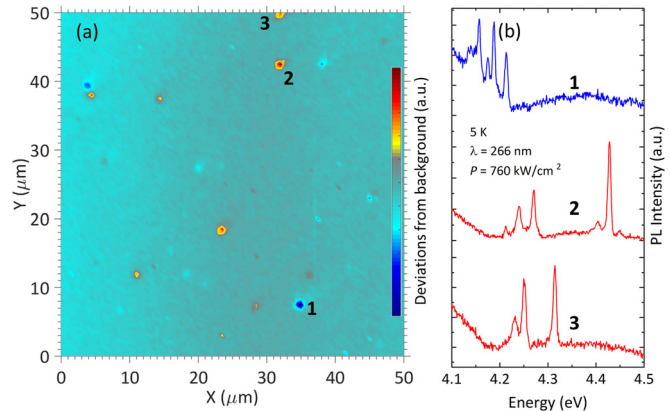


**FIG. 5.** (a)  $50 \times 50 \mu\text{m}^2$   $\mu$ -PL map. We plot deviations from the substrate background luminescence. (b) Selected sites from the map displaying the typical QD emission (vertically shifted for clarity) found throughout the sample.

assumption, we derive a density of active QD emitters within the energy interval of 3.7 to 4.5 eV of  $8 \times 10^6 \text{ cm}^{-2}$ . Clearly, this density only represents a lower boundary for the QD density, as particularly faint QD emitters could be masked by, e.g., the defect luminescence of the AlN substrate. Nevertheless, the present  $\mu$ -PL results of Fig. 5(a) in combination with the applied growth parameters suggest that the QD density is significantly lower than for the sample shown in AFM image 3 in Fig. 4 ( $4 \times 10^8 \text{ cm}^{-2}$ ). The luminescence of the wetting layer is discussed in the [supplementary material](#).

Currently, the defect luminescence of the bulk AlN substrate prevents any more sophisticated  $\mu$ -PL spectroscopy on single GaN QDs as, e.g.,  $g^{(2)}$ -measurements in order to ensure single photon emission characteristics. PL excitation spectroscopy of Alden *et al.* has shown that the AlN defect luminescence exhibits a distinct excitation channel at 4.7 eV.<sup>46</sup> Collazo *et al.* reported a corresponding absorption coefficient ( $\alpha_{4.7\text{eV}}$ ) above  $1000 \text{ cm}^{-1}$  for the first generation of AlN substrates.<sup>47</sup> In contrast, the present study utilized the latest generation of AlN substrates exhibiting  $\alpha_{4.7\text{eV}} < 100 \text{ cm}^{-1}$ . Hence, the defect luminescence intensity drops by around one order of magnitude (not shown), rendering the emission of single QDs well comparable to the bulk defect luminescence bands, cf. Fig. 5(b). Future substrate development aiming for lower point defects is needed in order to enable more in-depth quantum-optical studies of SK GaN QD samples.

In conclusion, we demonstrated SK growth for GaN QDs on AlN using  $\text{NH}_3$ -MBE by carefully tuning the  $\text{NH}_3$  flow and the substrate temperature. As a result, QD density control was achieved similar to the seminal In(Ga)As/GaAs QD system. AFM images reveal a dot density variation from  $10^8$  to  $10^{11} \text{ cm}^{-2}$ . The use of low growth rates as well as of AlN single crystal substrates allowed us to optically address individual QDs. These results represent a promising advance towards the integration of single GaN QD operating at non-cryogenic temperatures into more complex photonic structures.<sup>2</sup>

See [supplementary material](#) for additional information regarding experimental details, low temperature QD growth, QD ripening, and the luminescence of the wetting layer.

The authors thank C. Amendola and H. Zhang for technical support and R. Butté for the critical reading of this manuscript. This work was supported by the Swiss National Science Foundation through Grant Nos. 200021E-15468 and 200020-162657 and by the Marie Skłodowska-Curie action “PhotoHeatEffect” (Grant No. 749565) within the European Union’s Horizon 2020 research and innovation program.

## REFERENCES

- <sup>1</sup>G. Reithmaier, M. Kaniber, F. Flassig, S. Lichtmanecker, K. Müller, A. Andrejew, J. Vučković, R. Gross, and J. J. Finley, *Nano Lett.* **15**, 5208 (2015).
- <sup>2</sup>P. Lodahl, S. Mahmoodian, and S. Stobbe, *Rev. Mod. Phys.* **87**, 347 (2015).
- <sup>3</sup>J.-H. Kim, C. J. K. Richardson, R. P. Leavitt, and E. Waks, *Nano Lett.* **16**, 7061 (2016).
- <sup>4</sup>Y. Chen, J. Zhang, M. Zopf, K. Jung, Y. Zhang, R. Keil, F. Ding, and O. G. Schmidt, *Nat. Commun.* **7**, 10387 (2016).
- <sup>5</sup>M. Arcari, I. Söllner, A. Javadi, S. Lindskov Hansen, S. Mahmoodian, J. Liu, H. Thyrestrup, E. H. Lee, J. D. Song, S. Stobbe, and P. Lodahl, *Phys. Rev. Lett.* **113**, 093603 (2014).
- <sup>6</sup>P. Schnauber, J. Schall, S. Bounouar, T. Höhne, S.-I. Park, G.-H. Ryu, T. Heindel, S. Burger, J.-D. Song, S. Rodt, and S. Reitzenstein, *Nano Lett.* **18**, 2336 (2018).
- <sup>7</sup>A. Crespi, R. Ramponi, R. Osellame, L. Sansoni, I. Bongioanni, F. Sciarrino, G. Vallone, and P. Mataloni, *Nat. Commun.* **2**, 566 (2011).
- <sup>8</sup>F. Najafi, J. Mower, N. C. Harris, F. Bellei, A. Dane, C. Lee, X. Hu, P. Kharel, F. Marsili, S. Assefa, K. K. Berggren, and D. Englund, *Nat. Commun.* **6**, 5873 (2015).
- <sup>9</sup>A. Schliwa, M. Winkelnkemper, A. Lochmann, E. Stock, and D. Bimberg, *Phys. Rev. B* **80**, 161307 (2009).
- <sup>10</sup>S. Castelletto, B. C. Johnson, V. Ivády, N. Stavrias, T. Umeda, A. Gali, and T. Ohshima, *Nat. Mater.* **13**, 151 (2014).
- <sup>11</sup>N. Mizuochi, T. Makino, H. Kato, D. Takeuchi, M. Ogura, H. Okushi, M. Nothhaft, P. Neumann, A. Gali, F. Jelezko, J. Wrachtrup, and S. Yamasaki, *Nat. Photonics* **6**, 299 (2012).
- <sup>12</sup>P. Michler, A. Imamoglu, M. D. Mason, P. J. Carson, G. F. Strouse, and S. K. Buratto, *Nature* **406**, 968 (2000).
- <sup>13</sup>G. Hönig, G. Callsen, A. Schliwa, S. Kalinowski, C. Kindel, S. Kako, Y. Arakawa, D. Bimberg, and A. Hoffmann, *Nat. Commun.* **5**, 5721 (2014).
- <sup>14</sup>M. Holmes, S. Kako, K. Choi, P. Podemski, M. Arita, and Y. Arakawa, *Phys. Rev. Lett.* **111**, 057401 (2013).
- <sup>15</sup>G. Callsen, A. Carmele, G. Hönig, C. Kindel, J. Brunmeier, M. R. Wagner, E. Stock, J. S. Reparaz, A. Schliwa, S. Reitzenstein, A. Knorr, A. Hoffmann, S. Kako, and Y. Arakawa, *Phys. Rev. B* **87**, 245314 (2013).
- <sup>16</sup>M. J. Holmes, K. Choi, S. Kako, M. Arita, and Y. Arakawa, *Nano Lett.* **14**, 982 (2014).
- <sup>17</sup>S. Kako, M. Holmes, S. Sergent, M. Bürger, D. J. As, and Y. Arakawa, *Appl. Phys. Lett.* **104**, 011101 (2014).
- <sup>18</sup>D. Leonard, K. Pond, and P. M. Petroff, *Phys. Rev. B* **50**, 11687 (1994).
- <sup>19</sup>V. A. Shchukin and D. Bimberg, *Rev. Mod. Phys.* **71**, 1125 (1999).
- <sup>20</sup>B. Alloing, C. Zinoni, V. Zwiller, L. H. Li, C. Monat, M. Gobet, G. Buchs, A. Fiore, E. Pelucchi, and E. Kapon, *Appl. Phys. Lett.* **86**, 101908 (2005).
- <sup>21</sup>C. Adelman, B. Daudin, R. A. Oliver, G. A. D. Briggs, and R. E. Rudd, *Phys. Rev. B* **70**, 125427 (2004).
- <sup>22</sup>F. Widmann, J. Simon, B. Daudin, G. Feuillet, J. L. Rouvière, N. T. Pelekanos, and G. Fishman, *Phys. Rev. B* **58**, R15989 (1998).
- <sup>23</sup>J. Brown, F. Wu, P. M. Petroff, and J. S. Speck, *Appl. Phys. Lett.* **84**, 690 (2004).
- <sup>24</sup>B. Daudin, *J. Phys. Condens. Matter* **20**, 473201 (2008).
- <sup>25</sup>B. Damilano, N. Grandjean, F. Semond, J. Massies, and M. Leroux, *Appl. Phys. Lett.* **75**, 962 (1999).
- <sup>26</sup>B. Damilano, J. Brault, and J. Massies, *J. Appl. Phys.* **118**, 24304 (2015).
- <sup>27</sup>S. Sergent, B. Damilano, T. Huault, J. Brault, M. Korytov, O. Tottereau, P. Vennéguès, M. Leroux, F. Semond, and J. Massies, *J. Appl. Phys.* **109**, 053514 (2011).
- <sup>28</sup>V. G. Mansurov, Y. G. Galitsyn, A. Y. Nikitin, K. S. Zhuravlev, and P. Vennéguès, *Phys. Status Solidi* **3**, 1548 (2006).
- <sup>29</sup>D. Simeonov, A. Dussaigne, R. Butté, and N. Grandjean, *Phys. Rev. B* **77**, 075306 (2008).
- <sup>30</sup>M. Miyamura, K. Tachibana, and Y. Arakawa, *Appl. Phys. Lett.* **80**, 3937 (2002).
- <sup>31</sup>D. Simeonov, E. Feltn, J.-F. Carlin, R. Butté, M. Ilegems, and N. Grandjean, *J. Appl. Phys.* **99**, 083509 (2006).
- <sup>32</sup>J. Schmidt, C. Berger, P. Veit, S. Metzner, F. Bertram, J. Bläsing, A. Dadgar, A. Strittmatter, J. Christen, G. Callsen, S. Kalinowski, and A. Hoffmann, *Appl. Phys. Lett.* **106**, 252101 (2015).
- <sup>33</sup>J. M. Woodward, A. Y. Nikiforov, K. F. Ludwig, and T. D. Moustakas, *J. Appl. Phys.* **122**, 065305 (2017).
- <sup>34</sup>J. S. Brown, G. Koblmüller, R. Averbek, H. Riechert, and J. S. Speck, *J. Appl. Phys.* **99**, 124909 (2006).
- <sup>35</sup>N. Gogneau, D. Jalabert, E. Monroy, T. Shibata, M. Tanaka, and B. Daudin, *J. Appl. Phys.* **94**, 2254 (2003).
- <sup>36</sup>B. Borisov, S. Nikishin, V. Kuryatkov, and H. Temkin, *Appl. Phys. Lett.* **87**, 191902 (2005).
- <sup>37</sup>T. Huault, J. Brault, F. Natali, B. Damilano, D. Lefebvre, L. Nguyen, M. Leroux, and J. Massies, *Appl. Phys. Lett.* **92**, 51911 (2008).
- <sup>38</sup>S. Tamariz, D. Martin, and N. Grandjean, *J. Cryst. Growth* **476**, 58 (2017).
- <sup>39</sup>I. Bryan, Z. Bryan, S. Mita, A. Rice, J. Tweedie, R. Collazo, and Z. Sitar, *J. Cryst. Growth* **438**, 81 (2016).
- <sup>40</sup>H. Mariette, *C. R. Phys.* **6**, 23 (2005).
- <sup>41</sup>P. Sohi, D. Martin, and N. Grandjean, *Semicond. Sci. Technol.* **32**, 075010 (2017).
- <sup>42</sup>N. Grandjean, J. Massies, F. Semond, S. Y. Karpov, and R. A. Talalaev, *Appl. Phys. Lett.* **74**, 1854 (1999).
- <sup>43</sup>J. L. Rouvière, J. Simon, N. Pelekanos, B. Daudin, and G. Feuillet, *Appl. Phys. Lett.* **75**, 2632 (1999).
- <sup>44</sup>N. Gmeinwieser and U. T. Schwarz, *Phys. Rev. B* **75**, 245213 (2007).
- <sup>45</sup>W. Liu, J.-F. Carlin, N. Grandjean, B. Deveaud, and G. Jacopin, *Appl. Phys. Lett.* **109**, 042101 (2016).
- <sup>46</sup>D. Alden, J. S. Harris, Z. Bryan, J. N. Baker, P. Reddy, S. Mita, G. Callsen, A. Hoffmann, D. L. Irving, R. Collazo, and Z. Sitar, *Phys. Rev. Appl.* **9**, 054036 (2018).
- <sup>47</sup>R. Collazo, J. Xie, B. E. Gaddy, Z. Bryan, R. Kirste, M. Hoffmann, R. Dalmau, B. Moody, Y. Kumagai, T. Nagashima, Y. Kubota, T. Kinoshita, A. Koukitu, D. L. Irving, and Z. Sitar, *Appl. Phys. Lett.* **100**, 191914 (2012).